September 22, 2005

Matter-wave solitons of collisionally inhomogeneous condensates

G. Theocharis
P. Schmelcher
Panos Kevrekidis, *UMASS, Amherst*
D. J. Frantzeskakis

Matter-wave solitons of collisionally inhomogeneous condensates

G. Theocharis,[1,4] P. Schmelcher,[1,2] P. G. Kevrekidis,[3] and D. J. Frantzeskakis[4]
[1]*Theoretische Chemie, Physikalisch-Chemisches Institut, Im Neuenheimer Feld 229, Universität Heidelberg, 69120 Heidelberg, Germany*
[2]*Physikalisches Institut, Philosophenweg 12, Universität Heidelberg, 69120 Heidelberg, Germany*
[3]*Department of Mathematics and Statistics, University of Massachusetts, Amherst, Massachusetts 01003-4515, USA*
[4]*Department of Physics, University of Athens, Panepistimiopolis, Zografos, Athens 157 84, Greece*
(Received 26 April 2005; published 22 September 2005)

We investigate the dynamics of matter-wave solitons in the presence of a spatially varying atomic scattering length and nonlinearity. The dynamics of bright and dark solitary waves is studied using the corresponding Gross-Pitaevskii equation. The numerical results are shown to be in very good agreement with the predictions of the effective equations of motion derived by adiabatic perturbation theory. The spatially dependent nonlinearity is found to lead to a gravitational potential, as well as to a renormalization of the parabolic potential coefficient. This feature allows one to influence the motion of fundamental as well as higher-order solitons.

DOI: 10.1103/PhysRevA.72.033614 PACS number(s): 03.75.Lm, 05.45.Yv

I. INTRODUCTION

Recent years have seen enormous progress with respect to our understanding and the controlled processing of atomic Bose-Einstein condensates (BEC's) [1] both in theory and in experiment. In the case of nonlinear excitations, specifically solitons, the experimental observation of dark [2], bright [3,4], and gap [5] solitons has inspired many studies on matter-wave solitons in general. Apart from a fundamental interest in their behavior and properties, solitons are potential candidates for applications since there are possibilities to coherently manipulate them in matter-wave devices, such as atom chips [6]. Moreover, the formal similarities between matter-wave and optical solitons indicate that the former may be used in future applications similarly to their optical siblings, which have a time-honored history in optical fibers and waveguides (see, e.g., the recent reviews [7,8]).

Typically dark (bright) matter-wave solitons are formed in atomic condensates with repulsive (attractive) interatomic interactions—i.e., for atomic species with positive (negative) scattering length a. One of the very interesting aspects for tailoring and designing the properties of (atomic or molecular) BEC's is the possibility to control the interaction of ground-state species by changing the atomic collision dynamics and consequently changing either the sign or magnitude of the scattering length. A prominent way to achieve this is to apply an external magnetic field which provides control over the scattering length because of the rapid variation in collision properties associated with a threshold scattering resonance being a Feshbach resonance (see Refs. [9–11] and references therein). For low-dimensional setups a complementary way of tuning the scattering length or the nonlinear coupling at will is to change the transversal confinement in order to achieve an effective nonlinearity parameter for the dynamics in, e.g., the axial direction. In the limit of very strong transversal confinement this leads to the so-called confinement-induced resonance at which the modified scattering length diverges [12]. A third alternative approach uses the possibility of tuning the scattering length with an optically induced Feshbach resonance [13]. Varying the interactions and collisional properties of the atoms was crucial for a variety of experimental discoveries such as the formation of molecular BEC's [14] or the revelation of the BEC-BCS crossover [15]. Recent theoretical studies have predicted that a time-dependent modulation of the scattering length can be used to prevent collapse in higher-dimensional attractive BEC's [16] or to create robust matter-wave solitons [17].

Given the increasing degree of control with respect to the processing of BEC's it is nowadays "not only" possible to change the scattering length in the same way for the complete ultracold atomic ensemble—i.e., it can be tuned globally—but it is possible to obtain a locally varying scattering length thereby providing a variation of the collisional dynamics across the condensate. According to the above, this can be implemented by a (longitudinally) changing transversal confinement or an inhomogeneity of the external magnetic field in the vicinity of a Feshbach resonance. Very few investigations of condensates have addressed the presence of such an inhomogeneous environment [18,19].

To substantiate the above, let us specify in some more detail the case of a magnetically tuned scattering length. The behavior of the scattering length near a Feshbach resonant magnetic field B_0 is typically of the form $a(B)=\tilde{a}[1-\Delta/(B-B_0)]$, where $\tilde{a}$ is the value of the scattering length far from resonance and Δ represents the width of the resonance (see, e.g., [20]). Let us consider a quasi-one-dimensional (quasi-1D) condensate along the x direction exposed to a bias field B_1 sufficiently far from the resonant value B_0 in the presence of an additional gradient ϵ of the field; i.e., we have $B=B_1+\epsilon x$ (without loss of generality we take $\epsilon>0$), such that $B_1>B_0+\Delta$ or $B_1<B_0-\Delta$. Assuming $\epsilon x/(B_1-B_0)\ll 1$ for all values of x in the interval $(-L/2,L/2)$, where L is the characteristic spatial scale on which the evolution of the condensate takes place, it is readily seen that the scattering length can be well approximated by the spatially dependent form $a(x)=a_0+a_1x$, where $a_0=\tilde{a}[1-\Delta/(B_1-B_0)]$ and $a_1=\epsilon\Delta\tilde{a}/(B_1-B_0)^2$. In the following we will assume that a_0 and a_1 are of the same sign.

This opens the perspective of studying collisionally inhomogeneous condensates. In this work, we provide a first step

in this direction by investigating the behavior of nonlinear excitations, specifically bright and dark matter-wave solitons in attractive and repulsive quasi-1D BEC's, in the presence of a spatially dependent scattering length and nonlinearity. We investigate the soliton dynamics in different setups and analyze the impact of the spatially varying nonlinearity by numerically integrating the Gross-Pitaevskii (GP) equation as well as in the framework of adiabatic perturbation theory for solitons [21,22]. Being the first of its kind, the present work demonstrates that trapped condensates in an environment with spatially varying collisional interactions show a variety of different behaviors and properties. A prominent such example is the generation of a gravitational effective potential, as well as the renormalization of the harmonic potential prefactor, which may, in turn, lead to expulsive effective potentials for the solitary waves, even under trapping conditions. We believe that this study may pave the way for further investigations and emergent properties and applications of such settings that will be substantially different from the ones of collisionally homogeneous condensates.

The paper is organized as follows: In Sec. II the effective perturbed nonlinear Schrödinger (NLS) equation is derived. In Sec. III fundamental and higher-order soliton dynamics are considered and Bloch oscillations in the additional presence of an optical lattice are studied. Section IV is devoted to the study of dark matter-wave solitons, and in Sec. V the main findings of this work are summarized.

II. PERTURBED NLS EQUATION

It is widely known that at sufficiently low temperatures the evolution of a BEC is governed by the GP equation [1]

$$i\hbar\frac{\partial\psi}{\partial t} = -\frac{\hbar^2}{2m}\nabla^2\psi + V(\mathbf{r})\psi + g|\psi|^2\psi, \tag{1}$$

where $\psi(\mathbf{r},t)$ is the macroscopic wave function of the condensate, $V(\mathbf{r})=(m/2)(\omega_\perp^2 r_\perp^2+\omega_x^2 x^2)$ (with $r_\perp^2=y^2+z^2$) is the trapping potential, and m is the atomic mass, while $\omega_\perp$ and ω_x are the trapping frequencies in the transverse and longitudinal directions, respectively. Finally, the parameter $g=4\pi\hbar^2 a/m$ characterizes the two-particle interaction, with a being the s-wave scattering length, which is positive (negative) for repulsive (attractive) condensates consisting of, e.g., ^{23}Na or ^{87}Rb (^{85}Rb or ^{7}Li) atoms. Assuming a highly anisotropic ("cigar-shaped") trap with $\omega_x \ll \omega_\perp$, we seek solutions of Eq. (1) in the form [23]

$$\psi(\mathbf{r},t) = \Psi(x,t)\Phi(r_\perp)\exp(-i\gamma t), \tag{2}$$

where $\Phi(r)$ is a solution of the auxiliary problem for the quantum harmonic oscillator,

$$-\frac{\hbar^2}{2m}\nabla_\perp^2\Phi + \frac{1}{2}m\omega_\perp^2 r_\perp^2\Phi - \gamma\Phi = 0, \tag{3}$$

which, in the ground state, takes the form $\Phi(r_\perp)=\pi^{-1/2}l_\perp\exp(-r_\perp^2/2l_\perp^2)$, where $l_\perp=\sqrt{\hbar/m\omega_\perp}$ is the transverse harmonic oscillator length. Substituting Eq. (2) into Eq. (1) and averaging the resulting equation in the $r_\perp$ direction (i.e., multiplying by $\Phi^\star$ and integrating with respect to $r_\perp$), we finally obtain the 1D GP equation

$$i\hbar\frac{\partial\Psi}{\partial t} = -\frac{\hbar^2}{2m}\frac{\partial^2\Psi}{\partial x^2} + V(x)\Psi + \tilde{g}|\Psi|^2\Psi, \tag{4}$$

where the nonlinearity coefficient $\tilde{g}$ has an effective 1D form—namely, $\tilde{g}=g/2\pi l_\perp^2=2\hbar a\omega_\perp$ and $V(x)=(1/2)m\omega_x^2x^2$.

As discussed in the Introduction we assume a collisionally inhomogeneous condensate—i.e., a spatially varying scattering length according to $a(x)=a_0+a_1x$ where a_0 and a_1 are both positive (negative) for repulsive (attractive) condensates. Thus, the function $a(x)$ can be expressed as $a(x)=sA(x)$, where $A(x)\equiv|a_0|+|a_1|x$ is a positive definite function (for $-L/2<x<L/2$, where L is the characteristic length for the evolution of the condensate) and $s=\mathrm{sgn}(a_0)=\pm1$ for repulsive and attractive condensates, respectively. We can then reduce the original GP equation (4) to a dimensionless form as follows: x is scaled in units of the healing length $\xi=\hbar/\sqrt{n_0\tilde{g}_0 m}$, t in units of ξ/c (where $c=\sqrt{n_0\tilde{g}_0/m}$ is the Bogoliubov speed of sound), the atomic density $n\equiv|\Psi|^2$ is rescaled by the peak density n_0, and energy is measured in units of the chemical potential of the system $\mu=\tilde{g}_0 n_0$; in the above expressions $\tilde{g}_0\equiv2\hbar a_0\omega_\perp$ corresponds to the constant (dc) value a_0 of the scattering length. This way, the following normalized GP equation is readily obtained:

$$i\frac{\partial\psi}{\partial t} = -\frac{1}{2}\frac{\partial^2\psi}{\partial x^2} + V(x)\psi + s\tilde{g}(x)|\psi|^2\psi, \tag{5}$$

where $V(x)=(1/2)\Omega^2x^2$ and the parameter $\Omega\equiv(2a_0n_0)^{-1}(\omega_x/\omega_\perp)$ determines the magnetic trap strength. Additionally, $\tilde{g}(x)=1+\delta x$ is a positive definite function and $\delta\equiv\epsilon\Delta\xi[(B_1-B_0)(B_1-B_0-\Delta)]^{-1}$ is the gradient.

Let us provide experimental parameters for a quasi-1D condensate, confined in a cigar-shaped trap, with the ratio of the confining frequencies, $\omega_x/\omega_\perp$, of order $O(10^{-2})$ (typically $\omega_\perp\sim100\omega_x\sim2\pi\times1500$ Hz). In such a case, we may assume that the condensate contains $N\sim10^3$ atoms, with a peak atomic density $n_0\approx10^8$ m^{-1}. Then, taking the scattering length a to be of the order of nanometer (e.g., $\tilde{a}=-21.2$ nm or $\tilde{a}=2.75$ nm for a ^{85}Rb or ^{23}Na condensate), it turns out that the normalized trap strength Ω is typically of order $O(10^{-2})$. Let us consider the particular case of the attractive ^{85}Rb condensate, in which the Feshbach resonant magnetic field is $B_0=155$ G and the width of the resonance is $\Delta=11.6$ G [11]. Assuming a bias magnetic field $B_1=175$ G and a field gradient $\epsilon\sim1$ G/μm, the spatially dependent scattering length $a(x)\equiv a_0+a_1x$ is characterized by the values $a_0=-8.9$ nm and $a_1=-0.6\times10^{-3}$. In such a case, the characteristic length L for the evolution of the condensate is allowed to be ~20 μm, so that the approximation $\epsilon x/(B_1-B_0)\ll1$ will be valid. In the framework of the normalized GP equation (5), the spatially dependent nonlinearity coefficient takes the form $\tilde{g}(x)=1+\delta x$, with $\delta\sim O(10^{-2})$ and $s=-1$. On the other hand, in the case of the repulsive ^{23}Na condensate, in which $B_0=907$ G and $\Delta=1$ G [10], we may assume that the bias field and the gradient are $B_1=885$ G and $\epsilon\sim3$ G/μm, respectively. In such a case, the respective values of the above-mentioned physical parameters are $a_0=2.87$ nm, $a_1=0.17\times10^{-4}$, $L\sim10$ μm, and $\delta\sim O(10^{-2})$. Similar setups can also be achieved for other condensate spe-

cies, such as the attractive ^{7}Li or the repulsive ^{87}Rb (see, e.g., a relevant discussion in Sec. III).

According to the above estimations based on typical experimental values of the physical parameters, it is clear that for sufficiently small values of the field gradient ϵ, the resulting normalized field gradient δ is also small and is of the order of the dimensionless magnetic trap strength Ω. Thus, Ω and δ are the natural small parameters of the problem.

We now introduce the transformation $\psi = u/\sqrt{g}$ to rewrite Eq. (5) in the following form:

$$i\frac{\partial u}{\partial t} + \frac{1}{2}\frac{\partial^2 u}{\partial x^2} - s|u|^2 u = R(u). \tag{6}$$

Apparently, Eq. (6) has the form of a perturbed NLS equation (of the focusing or defocusing type, for $s=-1$ and $s=+1$, respectively), with the perturbation $R(u)$ being given by

$$R(u) \equiv V(x)u + \frac{d}{dx}\ln(\sqrt{g})\frac{\partial u}{\partial x} + \frac{1}{2}\left[\frac{d^2}{dx^2}\ln(\sqrt{g}) - \left(\frac{d}{dx}\ln(\sqrt{g})\right)^2\right]u. \tag{7}$$

The last two terms on the right-hand side of Eq. (7) are of higher order with respect to the perturbation parameter δ than the second term and will henceforth be ignored (this will be discussed in more detail below). We therefore examine the soliton dynamics in the presence of the perturbation including the first two terms of Eq. (7).

III. BRIGHT MATTER-WAVE SOLITONS

A. Fundamental solitons

In the case $s=-1$ and in the absence of the perturbation, Eq. (6) represents the traditional focusing NLS equation, which possesses a commonly known family of fundamental bright soliton solutions of the form [24]

$$u(x,t) = \eta\,\mathrm{sech}[\eta(x-x_0)]\exp[i(kx-\phi(t))], \tag{8}$$

where η is the amplitude and inverse spatial width of the soliton, x_0 is the soliton center, the parameter $k=dx_0/dt$ defines both the soliton wave number and velocity, and finally $\phi(t)=(1/2)(k^2-\eta^2)t+\phi_0$ is the soliton phase (ϕ_0 being an arbitrary constant). Let us assume now that the soliton width η^{-1} is much smaller than $\Omega^{-1/2}$ and δ^{-1} [namely, the characteristic spatial scales of the trapping potential and the function $g(x)$] or, physically speaking, the potential $V(x)$ and function $g(x)$ vary little on the soliton scale. In this case, we may employ the adiabatic perturbation theory for solitons [21] to treat analytically the effect of the perturbation $R(u)$ on the soliton (8). According to this approach, the soliton parameters η, k, and x_0 become unknown, slowly varying functions of time t, but the functional form of the soliton [see Eq. (8)] remains unchanged. Then, from Eq. (6), it is found that the number of atoms, $N=\int_{-\infty}^{+\infty}|u|^2dx$, and the momentum $P=(i/2)\int_{-\infty}^{+\infty}[u(\partial u^\star/\partial x)-u^\star(\partial u/\partial x)]dx$, which are integrals of motion of the unperturbed system, evolve, in the presence of the perturbation, according to the equations

$$\frac{dN}{dt} = -2\,\mathrm{Im}\left[\int_{-\infty}^{+\infty} Ru^* dx\right], \tag{9}$$

$$\frac{dP}{dt} = 2\,\mathrm{Re}\left[\int_{-\infty}^{+\infty} R\frac{\partial u^*}{\partial x}dx\right]. \tag{10}$$

We remark that the true number of atoms, $\int_{-\infty}^{+\infty}|\psi|^2dx$, is conserved for Eq. (5) but the transformation leading to Eq. (6) no longer preserves that conservation law, leading, in turn, to Eq. (9).

We now substitute the ansatz (8) (but with the soliton parameters being functions of time) into Eqs. (9) and (10); furthermore, we use a Taylor expansion of the second term of Eq. (7), around $x=x_0$ (keeping the two leading terms). The latter expansion is warranted by the exponentional localization of the wave around $x=x_0$. We then obtain the evolution equations for $\eta(t)$ and $k(t)$,

$$\frac{d\eta}{dt} = k\eta\frac{\partial}{\partial x_0}\ln(g), \tag{11}$$

$$\frac{dk}{dt} = -\frac{\partial V}{\partial x_0} + \frac{\eta^2}{3}\frac{\partial}{\partial x_0}\ln(g). \tag{12}$$

To this end, recalling that $dx_0/dt=k$, we may combine Eqs. (11) and (12) to derive the following equation of motion for the soliton center:

$$\frac{d^2x_0}{dt^2} = -\frac{\partial V}{\partial x_0} + \frac{\eta^2(0)}{6g^2(0)}\left(\frac{\partial g^2}{\partial x_0}\right), \tag{13}$$

where $\eta(0)$ and $g(0)\equiv g(x_0(0))$ are the initial values of the amplitude and function $g(x)$, respectively. Notice that the above result indicates that the main contribution from the spatially dependent scattering length comes to order δ^2 [while the contribution of the last two terms in Eq. (7) would have been $O(\delta^3)$ and is neglected]. It is clear that in the particular case where $g(x)=1+\delta x$, Eq. (13) describes the motion of a unit mass particle in the presence of the effective potential

$$V_{\mathrm{eff}}(x_0) = \frac{1}{2}\omega_{bs}^2 x_0^2 - \beta x_0, \tag{14}$$

where the parameter β is defined as

$$\beta = \frac{\eta^2(0)\delta}{3[1+\delta x_0(0)]^2} \tag{15}$$

and

$$\omega_{\mathrm{bs}} = \sqrt{\Omega^2 - \delta\beta} \tag{16}$$

is the oscillation frequency of the bright soliton. In the absence of the spatial variation of the scattering length ($\delta=0$), Eq. (13) actually expresses the Ehrenfest theorem, implying that the bright soliton oscillates with a frequency $\omega_{bs}=\Omega$ in the presence of the harmonic potential with strength Ω. Nevertheless, the presence of the gradient modifies significantly the bright soliton dynamics as follows: First, as seen by the second term on the right-hand side of Eq. (14), apart from

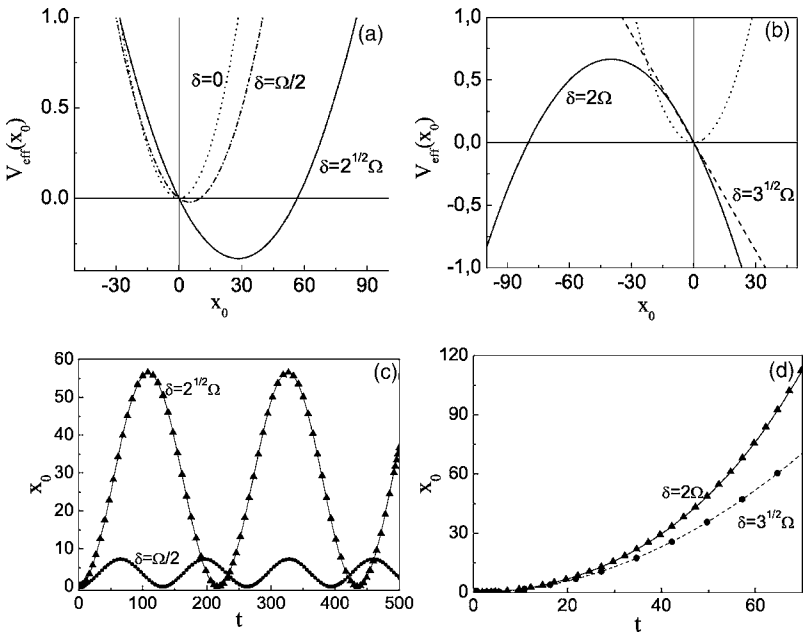

FIG. 1. Top panels: the effective potential $V(x_0)$ as a function of the soliton center x_0 for a trap strength $\Omega=0.05$ for a fundamental bright soliton of amplitude $\eta(0)=1$, initially placed at the trap center $[x_0(0)=0]$. Different values of the gradient modify the character of the potential: in panel (a) it is purely attractive ($\delta=0,\Omega/2,\sqrt{2}\Omega$), while in (b) it is either purely gravitational ($\delta=\sqrt{3}\Omega$) or expulsive ($\delta=2\Omega$). Bottom panels: evolution of the center of the bright soliton for the above cases: (c) for attractive effective potentials and (d) for gravitational or expulsive ones. The agreement between numerical results (solid and dashed lines) and the theoretical predictions (triangles, dots) is excellent.

the harmonic trapping potential, an effective gravitational potential is also present, which induces an acceleration of the initial soliton towards larger values of x_0 (for $\delta>0$); i.e., it shifts the center of the harmonic potential from $x_0=0$ to $x_0=\beta/\omega_{bs}^2$. Second, the oscillation frequency of the bright soliton is modified for $\delta\neq 0$, according to Eq. (16). Moreover, depending on the initial values of the parameters—namely, for $\beta\delta\geqslant\Omega^2$—an interesting situation may occur, in which the effective harmonic potential, instead of being purely attractive, can effectively disappear or be *expulsive*.

The solution to Eq. (13) in the variables $y_0=x_0-\beta/\omega_{bs}^2$ is, of course, a simple classical oscillator

$$y_0(t)=y_0(0)\cos(\omega_{bs}t)+\frac{\dot{y}_0(0)}{\omega_{bs}}\sin(\omega_{bs}t), \tag{17}$$

which is valid for $\omega_{bs}^2>0$. For $\omega_{bs}^2<0$ the trigonometric functions have to be replaced by hyperbolic ones. In the case $\omega_{bs}^2=0$, the resulting motion (to the order examined) is the one due to a uniform acceleration with $x_0(t)=x_0(0)+\dot{x}_0(0)t+(1/2)\beta t^2$.

The above analytical predictions have been confirmed by direct numerical simulations. In particular, we have systematically compared the results obtained from Eq. (13) with the results of the direct numerical integration of the GP equation (5). In the following, we use the trap strength $\Omega=0.05$, initial soliton amplitude $\eta(0)=1$, initial location of the soliton $x_0(0)=0$, and different values for the normalized gradient δ. The above values of the parameters may correspond to a ^{7}Li condensate containing $N\approx 4000$ atoms, confined in a quasi-1D trap with frequencies $\omega_x=2\pi\times 14$ Hz and $\omega_\perp=100\omega_x$. Note that these values correspond to a scattering length $a_0=-0.21$ nm (pertaining to a magnetic field of 425 G), a value for which a bright matter-wave soliton has been observed experimentally [4].

In Fig. 1(a), the original harmonic trapping potential $V(x)$ (dotted line, $\delta=0$) is compared to the effective potential modified by the presence of the gradient for $\delta=(1/2)\Omega$ (dashed line) and $\delta=\sqrt{2}\Omega$ (solid line). In these cases, the effective harmonic potential is attractive and the gradient displaces the equilibrium point to the right. Figure 1(b) shows the case $\delta=\sqrt{3}\Omega$ (dashed line) for which the effective harmonic potential is canceled, resulting in a purely gravitational potential. Also, upon suitably choosing the value of δ, e.g., for $\delta=2\Omega$ (solid line) the effective potential becomes expulsive. The dynamics of the bright matter-wave soliton pertaining to the above cases are shown in Figs. 1(c) (for the attractive effective potential) and 1(d) (for the gravitational or expulsive effective potential). In particular, in Fig. 1(c), it is clearly seen that the evolution of the soliton center x_0 is periodic, but with a larger amplitude and smaller frequency of oscillations, as compared to the respective case with $\delta=0$. The analytical predictions of Eq. (13)–(17) [triangles for $\delta=\sqrt{2}\Omega$ and dots for $\delta=(1/2)\Omega$] are in perfect agreement with the respective results obtained by direct numerical integration of the GP equation (5). On the other hand, as shown in Fig. 1(d), in the case of a gravitational or expulsive effective potential, the function $x_0(t)$ is monotonically increasing, with the analytical predictions being in excellent agreement with the numerical simulations. For a purely gravitational or expulsive effective potential, Eq. (11) shows that the amplitude (width) of the soliton increases (decreases) monotonically as well, which recovers the predictions of Ref. [18]. This type of evolution suggests that the bright soliton is compressed adiabatically in the presence of the gradient.

Before proceeding further, it is worth mentioning that, in principle, apart from the evolution of the soliton parameters (derived in the framework of the adiabatic approach in the perturbation theory for solitons), there also exists a radiation part contributed by the perturbation $R(u)$, which also needs to be considered. Nevertheless, generally speaking, it is known [21] (see also the more recent work [25]) that if the perturbation $R(u)$ is of the order of a small parameter—e.g., ϵ—then the density of the corresponding radiation part

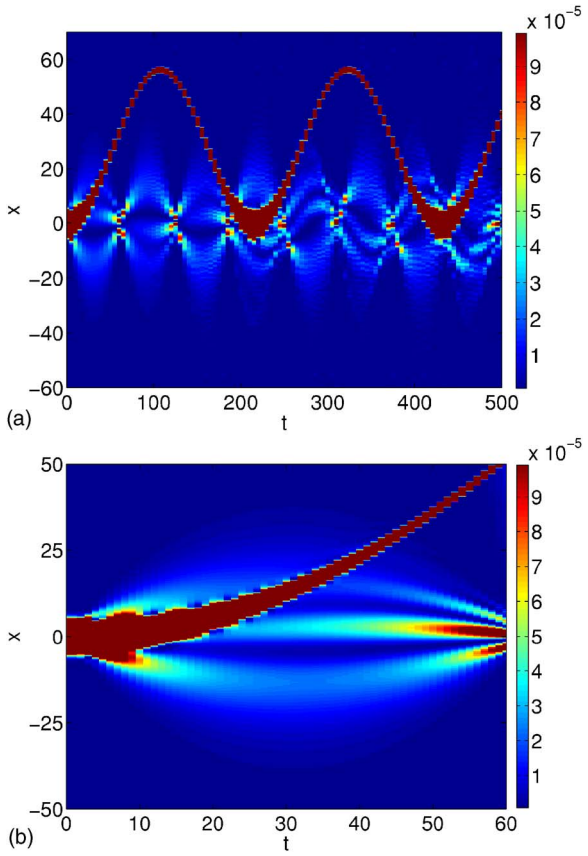

FIG. 2. (Color online) Spatiotemporal contour plots of the soliton densities for $\delta=\sqrt{2}\Omega$ (top panel) and $\delta=\sqrt{3}\Omega$ (bottom panel) up to a scale 10^{-4} (densities of 10^{-4} or greater are presented in dark red). In both cases $\Omega=0.05$. These contour plots correspond to an attractive or a gravitational effective potential respectively (see also Fig. 1). One can clearly observe the presence of the radiation emitted, which is detectable on a scale of 10^{-4}.

(which can be obtained in the second-order approximation of the perturbation theory) is of the order ϵ^2. In our case, as the respective small parameter (Ω or δ) is of the order $O(10^{-2})$, the density of the pertaining radiation is of the order of $O(10^{-4})$. This has been verified in our simulations, as is shown in Fig. 2. There, spatiotemporal contour plots of the soliton density, in the cases where the effective potential is either attractive (left panel of Fig. 2 for $\delta=\sqrt{2}\Omega$) or gravitational (right panel of Fig. 2 for $\delta=\sqrt{3}\Omega$), demonstrate that the radiation is indeed detectable on a scale of 10^{-4}. Note that the radiation is always confined due to the presence of the trapping potential and it is stronger in spatial regions where the soliton is wider: In such a case the soliton experiences in a stronger manner the presence of the inhomogeneity of the scattering length. According to the above discussion, it is clear that for such weak inhomogeneous perturbations the radiation emitted by the matter-wave soliton can safely be neglected. Finally, the above arguments also explain the excellent agreement between the analytical results based on the adiabatic approach of the perturbation theory and the direct numerical integration of the GP equation. Clearly, a systematic study of the the full problem concerning the evolution of the soliton and concomitant radiation is beyond the scope of this work.

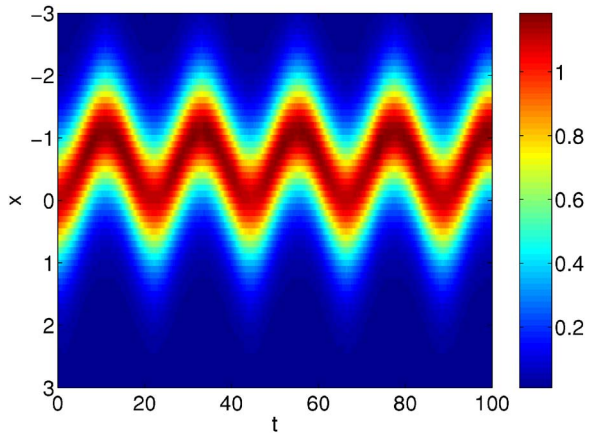

FIG. 3. (Color online) Spatiotemporal contour plot of the soliton density for $\Omega=0.075$, $\delta=\sqrt{3}\Omega$, and an optical lattice with $V_0=0.25$ and $\kappa=0.5$. One can clearly discern the presence of Bloch oscillations in the evolution of the density, whose period is in very good agreement with the corresponding theoretical prediction.

Let us consider another setup which combines the "effective" linear potential with an external harmonic and a periodic trap:

$$V(x)=\frac{1}{2}\Omega^2x^2+V_0\sin^2(\kappa x). \tag{18}$$

The periodic potential in Eq. (18) can be obtained experimentally by superimposing two counterpropagating laser beams. It is well known that the dynamics in the combined presence of a (effective) linear and a periodic potential results in the so-called Bloch oscillations (for a recent discussion of the relevant phenomenology and bibliography see, e.g., [26]). These oscillations occur due to the interplay of the linear and periodic potential with a definite period $T=2\kappa/\beta$ [26]. We have examined numerically this analytical prediction in the presence of an optical lattice potential with $V_0=0.25$ and $k=0.5$. The numerical evaluation of the period of the soliton motion in the combined potential is $T\approx 22.15$, less than 4% off the corresponding theoretical prediction. The time-periodic evolution of the soliton is shown in the spatiotemporal contour plot of Fig. 3.

B. Higher-order solitons

Apart from the fundamental bright soliton in Eq. (8), it is well known [27] that specific $\mathcal{N}$-soliton exact solutions in the unperturbed NLS equation [Eq. (6) with $s=-1$ and $R=0$] are generated by the initial condition $u(x,0)=A\,\mathrm{sech}(x)$ (for $\eta=1$), and the soliton amplitude A is such that $A-1/2<\mathcal{N}\leqslant A+1/2$ to excite a soliton of order $\mathcal{N}$. The exact form of the $\mathcal{N}$ soliton is cumbersome and will not be provided here; nevertheless, it is worth noticing some features of these solutions: First, the number of atoms of the $\mathcal{N}$th soliton is $\mathcal{N}^2$ times the one of the fundamental soliton and second, for any $\mathcal{N}$, the soliton solution is periodic with the intrinsic frequency of the shape oscillations being $\omega_{\mathrm{intr}}=4\eta^2$. We now examine the dynamics of the $\mathcal{N}$-soliton solution in the presence of the spatially varying nonlinearity.

We have performed numerical simulations in the case of the so-called double ($\mathcal{N}=2$) bright soliton solution with initial soliton amplitude $A=2.5$. In the absence of the gradient ($\delta=0$), if the soliton is placed at the trap center ($x_0=0$, with x_0 being the soliton center), it only executes its intrinsic oscillations with the above-mentioned frequency ω_{intr}. On the other hand, if the soliton is displaced ($x_0\neq 0$), apart from its internal vibrations, it performs oscillations governed by the simple equation $\ddot{x}_0+\Omega^2 x_0=0$, in accordance to the Kohn theorem (see [28,29] for an application in the context of bright matter-wave solitons). Nevertheless, for $\delta\neq 0$, the double soliton (initially placed at the trap center), contrary to the previous case, splits into two single solitons, with different amplitudes due to the effective gravity discussed in the case of the fundamental soliton. Due to the effective gravitational force, the soliton moving to the right (see, e.g., Fig. 4) is the one with the larger amplitude (and velocity) and is more mobile than the one moving to the left (which has the smaller amplitude).

As each of these two solitons is close to a fundamental one, their subsequent dynamics (after splitting) may be understood by means of the effective equations of motion derived in the previous section. In particular, depending on the values of the relevant parameters involved in Eq. (14) [$\eta(0)$ is now the amplitude of each soliton after splitting] the solitons may both be trapped, or may escape (either one or both of them), if the effective potential is expulsive. In the former case, both solitons perform oscillations (in the presence of the effective attractive potential) and an example is shown in Fig. 4 (for $\Omega=0.1$, $\delta=0.01$). Note that the center of mass of the ensemble oscillates with a period $T=2\pi/\Omega=62.8$ (which is in accordance with Kohn's theorem). During the evolution, as each of the two solitons oscillate in the trap with different frequencies, they may undergo a head-on collision (see, e.g., bottom panel of Fig. 4 at $t\approx 55$). It is clear that such a collision is nearly elastic, with the interaction between the two solitons being repulsive.

Importantly, for smaller values of the trap strength Ω, we have found that it is possible to release either one or both solitons from the trap: In particular, for $\Omega=0.05$ and $\delta=0.025$, we have found that the large-amplitude soliton escapes the trap, while the small-amplitude one performs oscillations. On the other hand, for the same value of the trap strength but for $\delta=0.05$ both solitons experience an expulsive effective potential and thus both escape from the trap. It is therefore in principle possible to use the spatially varying nonlinearity not only to split a higher-order bright soliton to a chain of fundamental ones, but also to control the trapping or escape of the resulting individual fundamental solitons.

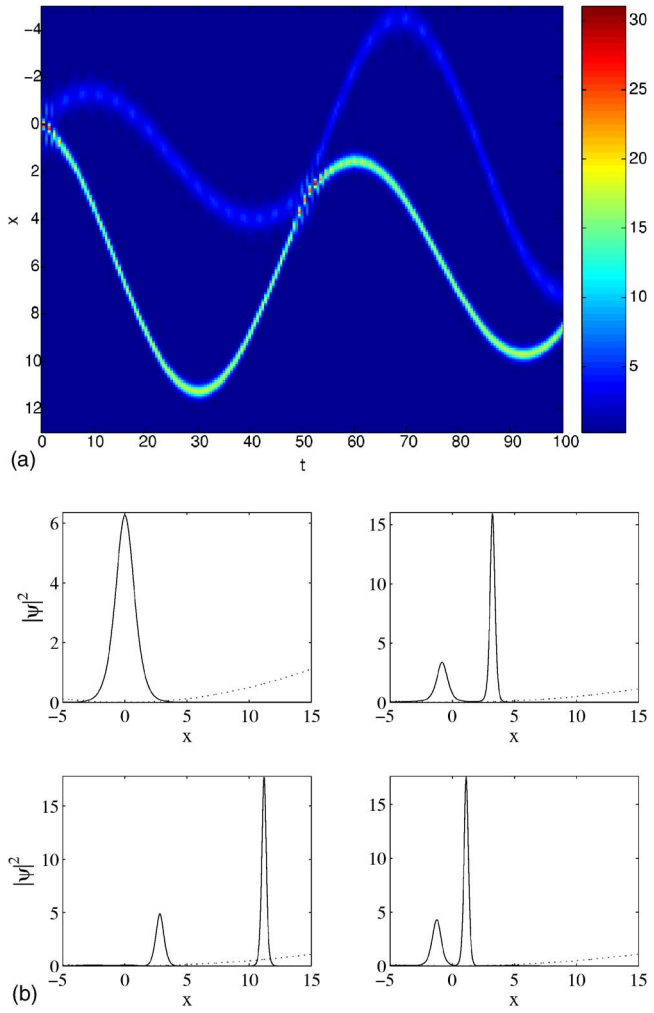

FIG. 4. (Color online) Evolution of a double soliton with initial amplitude $A=2.5$ initially placed at the trap center ($x=0$) with a strength $\Omega=0.1$ in the presence of a gradient $\delta=0.01$. Top panel: spatiotemporal contour plot of the density. Bottom panels: snapshots of the evolution of the density are shown for $t=0$ (top left panel), $t=10$ (top right panel), $t=30$ (bottom left panel), and $t=60$ (bottom right panel), covering almost one period of the oscillation. Dashed lines correspond to the trapping potential.

IV. DARK MATTER-WAVE SOLITONS

We now turn to the dynamics of dark matter-wave solitons in the framework of Eq. (5) for $s=+1$ (i.e., the defocusing case of condensates with repulsive interactions). First, we examine the equation governing the background wave function. The latter is taken in the form $\psi=\Phi(x)\exp(-i\mu t)$ (μ being the chemical potential) and the unknown background wave function $\Phi(x)$ satisfies the real equation

$$\mu\Phi=-\frac{1}{2}\frac{d^2\Phi}{dx^2}+V(x)\Phi+g(x)\Phi^3. \tag{19}$$

To describe the dynamics of a dark soliton on top of the inhomogeneous background satisfying Eq. (19), we introduce the ansatz (see, e.g., [30])

$$\psi=\Phi(x)\exp(-i\mu t)v(x,t) \tag{20}$$

into Eq. (5), where the unknown wave function $v(x,t)$ represents a dark soliton. This way, employing Eq. (19), the following evolution equation for the dark soliton wave function is readily obtained:

$$i\frac{\partial v}{\partial t}+\frac{1}{2}\frac{\partial^2 v}{\partial x^2}-g\Phi^2(|v|^2-1)v=-\frac{d}{dx}\ln(\Phi)\frac{\partial v}{\partial x}. \quad (21)$$

Taking into account that in the framework of the Thomas-Fermi (TF) approximation [1] a simple solution of Eq. (19) is expressed as

$$\Phi(x)=\sqrt{\max\left[\frac{\mu-V(x)}{g(x)},0\right]}, \quad (22)$$

Eq. (21) can be simplified to the defocusing perturbed NLS equation

$$i\frac{\partial v}{\partial t}+\frac{1}{2}\frac{\partial^2 v}{\partial x^2}-\mu(|v|^2-1)v=Q(v), \quad (23)$$

where the perturbation $Q(v)$ has the form

$$Q(v)=(1-|v|^2)vV+\frac{1}{2(\mu-V)}\frac{dV}{dx}\frac{\partial v}{\partial x}+\frac{d}{dx}[\ln(\sqrt{g})]\frac{\partial v}{\partial x}, \quad (24)$$

and higher-order perturbation terms have once again been neglected. In the absence of the perturbation, Eq. (23) represents the completely integrable defocusing NLS equation, which has a dark soliton solution of the form [31] (for $\mu=1$)

$$v(x,t)=\cos\varphi\tanh\zeta+i\sin\varphi, \quad (25)$$

where $\zeta\equiv\cos\varphi[x-(\sin\varphi)t]$, while $\cos\varphi$ and $\sin\varphi$ are the soliton amplitude and velocity, respectively, φ being the so-called soliton phase angle ($|\phi|\leqslant\pi/2$). To treat analytically the effect of the perturbation (24) on the dark soliton, we employ the adiabatic perturbation theory devised in Ref. [22]. As in the case of bright solitons, according to this approach, the dark soliton parameters become slowly varying unknown functions of t, but the functional form of the soliton remains unchanged. Thus, the soliton phase angle becomes $\varphi\rightarrow\varphi(t)$ and, as a result, the soliton coordinate becomes $\zeta\rightarrow\zeta=\cos\varphi(t)[x-x_0(t)]$, where

$$x_0(t)=\int_0^t\sin\varphi(t')dt' \quad (26)$$

is the soliton center. Then, the evolution of the parameter φ, governed by the equation [22]

$$\frac{d\varphi}{dt}=\frac{1}{2\cos^2\varphi\sin\varphi}\mathrm{Re}\left[\int_{-\infty}^{+\infty}Q(v)\frac{\partial v^*}{\partial t}dx\right], \quad (27)$$

leads (through similar calculations and Taylor expansions as for the bright soliton case) to the result

$$\frac{d\phi}{dt}=-\cos\varphi\left[\frac{1}{2}\frac{\partial V}{\partial x_0}+\frac{1}{3}\frac{\partial}{\partial x_0}\ln(g)\right]. \quad (28)$$

To this end, combining Eqs. (26) and (28), we obtain the corresponding equation of motion for the soliton center,

$$\frac{d^2x_0}{dt^2}=-\frac{1}{2}\frac{\partial V}{\partial x_0}-\frac{1}{3}\frac{\partial}{\partial x_0}\ln(g), \quad (29)$$

in which we have additionally assumed nearly stationary dark solitons with $\cos\varphi\approx1$. As in the case of bright solitons, the validity of Eq. (29) does not rely on the specific form of $g(x)$, as long as this function (and the trapping potential) are slowly varying on the dark soliton scale (i.e., the healing length). In the particular case with $g(x)=1+\delta x$, Eq. (29) describes the motion of a unit mass particle in the presence of the effective potential

$$W_{\mathrm{eff}}(x_0)=\frac{1}{4}\Omega^2x_0^2+\frac{1}{3}\ln(1+\delta x_0). \quad (30)$$

For $\delta=0$, Eq. (29) implies that the dark soliton oscillates with a frequency $\Omega/\sqrt{2}$ in the harmonic potential with strength Ω [30,32–34]. However, in the presence of the gradient and for sufficiently small δ, Eq. (30) implies the following: First, the oscillation frequency ω_{ds} of the dark soliton is downshifted in the presence of the linear spatial variation of the scattering length, according to

$$\omega_{\mathrm{ds}}=\sqrt{\frac{1}{2}\Omega^2-\frac{1}{3}\delta^2}. \quad (31)$$

Additionally to the effective harmonic potential, the dark soliton dynamics is also modified by an effective gravitational potential ($\sim\delta x_0/3$), which induces an acceleration of the soliton towards larger values of x_0 (for $\delta>0$). It should be noted that as dark solitons behave as effective particles with negative mass, the effective gravitational force possesses a positive sign, while in the case of bright solitons (which have positive effective mass) it has the usual negative sign [see Eqs. (14) and (30)].

Direct numerical simulations confirm the above analytical findings. In particular, we consider an initially stationary dark soliton [with $\cos\varphi(0)=0$], placed at $x_0=0$, on top of a TF cloud [see Eq. (22)] characterized by a chemical potential $\mu=1$ (the trapping frequency is here $\Omega=0.05$). In the absence of the gradient such an initial dark soliton should be purely stationary. However, considering a gradient with $\delta=0.01$, it is clear that the TF cloud will become asymmetric, as shown in Fig. 5(a), and the soliton will start performing oscillations. The latter are shown in Fig. 5, where the analytical predictions (points) are directly compared to the results obtained by direct numerical integration of the GP equation (solid line). As is seen, the agreement between the two is very good; additionally, we note that the oscillation frequency found numerically is $2\pi/177$, while the respective theoretical prediction is $2\pi/180.7$, with the error being $\approx3\%$.

As discussed and analyzed above, the presented adiabatic perturbation theory is able to describe quite accurately the evolution of the dark soliton parameters. Nevertheless, as in the case of the bright solitons, this approach does not take into regard the radiation, in the form of sound waves, emitted by the soliton due to the presence of the inhomogeneity (in both the TF background and the nonlinearity coefficient). In the case considered above, the radiation is clearly visible in Fig. 5(c). Analytical results for the inhomogeneity-induced radiation of dark solitons oscillating on top of the TF cloud have been obtained in [33], but for small-amplitude dark solitons that can be described by an effective Korteweg–de Vries equation. However, such an approximation cannot be

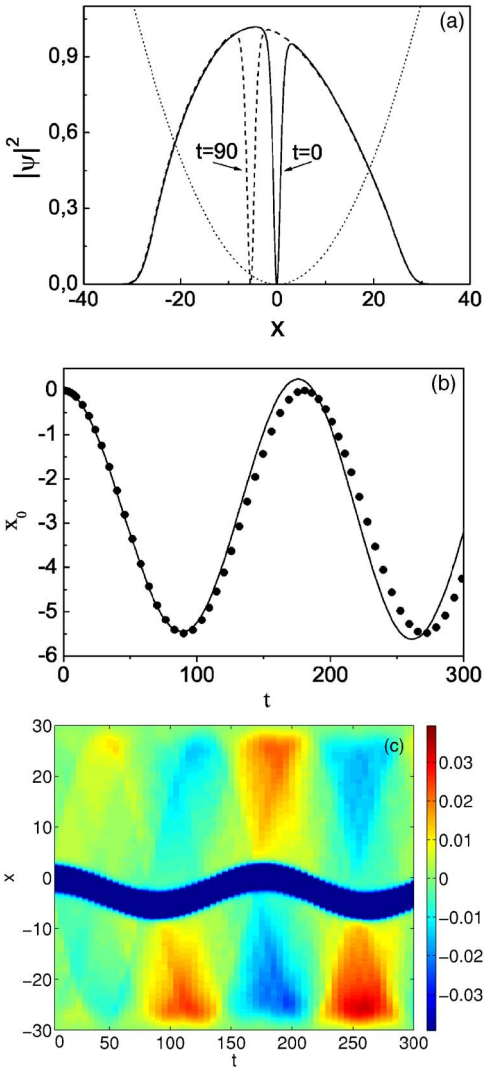

FIG. 5. (Color online) (a) Two snapshots of the density of the dark soliton (at $t=0$ and $t=90$) on top of a Thomas-Fermi cloud. The chemical potential is $\mu=1$, the trap strength is $\Omega=0.05$, and the gradient is $\delta=0.01$. (b) The motion of the center of a dark soliton. Solid line and dots correspond to the numerical integration of the GP equation and analytical predictions [see Eq. (29)], respectively. (c) Spatiotemporal contour plot of the reduced condensate density—i.e., the actual density (density of the Thomas-Fermi cloud with the dark soliton) minus the Thomas-Fermi density—demonstrating the radiation, in the form of sound waves, emitted by the dark soliton. The radiation is detectable on a scale of 10^{-2}.

adopted in our case, as we deal with nearly black solitons moving in a vicinity of the center of the condensate. In principle, the analytical treatment of the radiation emitted by dark solitons of arbitrary amplitude, also in the presence of the inhomogeneous nonlinearity coefficient, can be given by means of a systematic asymptotic multiscale expansion method, recently devised in [35]. Note that in this latter work, it was shown that if the perturbation $Q(v)$ [see Eq. (23)] is of the order ϵ, then the density of the corresponding radiation part is of the same order ϵ; this means that the radiation emitted by the dark soliton is stronger as compared to the one for the bright soliton case. This result has been verified in the simulations, as shown in Fig. 5(c), where the radiation density is indeed detectable on a scale of 10^{-2} (for $\Omega=0.05$ and $\delta=0.01$). The approach of [35] may also be used to study the reflections of the soliton and the concomitant energy loss, as observed in other analytical [36] and numerical [37] studies. Although the study of the above issues is quite interesting in its own right, it clearly goes beyond the scope of this paper.

V. SUMMARY

We have analyzed the dynamics of bright and dark matter-wave solitons in quasi-1D BEC's characterized by a spatially varying nonlinearity. The formulation of the problem is based on a Gross-Pitaevskii equation with a spatially dependent scattering length induced, e.g., by a bias magnetic field near a Feshbach resonance augmented by a field gradient. The GP equation has been reduced to a perturbed nonlinear Schrödinger equation, which is then analyzed in the framework of the adiabatic approximation in the perturbation theory for solitons, treating them as quasiparticles. This way, effective equations of motion for the soliton centers (together with evolution equations for their other characteristics) were derived analytically. The analytical results were corroborated by direct numerical simulations of the underlying GP equations.

In the case of bright matter-wave solitons initially confined in a parabolic trapping potential, it is found that (depending on the values of the gradient and the initial soliton parameters) there is a possibility to switch the character of the effective potential from attractive to purely gravitational or expulsive. It has been thus demonstrated that a bright soliton can escape the trap and be adiabatically compressed. On the other hand, considering the additional presence of an optical lattice potential, it has been shown that in the case where the effective potential is purely gravitational, Bloch oscillations of the bright solitons are possible. Higher-order bright solitons have been shown to typically split in the presence of a spatially varying nonlinearity into fundamental ones, whose subsequent dynamics is determined by the properties of the resulting single-soliton splinters. In the case of dark matter-wave solitons, the relevant background—i.e., the Thomas-Fermi cloud—is modified by the inhomogeneous nonlinearity. The dynamics of the dark solitons follows a Newtonian equation of motion for a particle with a negative effective mass, and the oscillation frequency of the dark solitons has been derived analytically. The latter is always downshifted as compared to the oscillation frequency pertaining to a spatially constant scattering length. Thus, generally speaking, the presented results show that a spatial inhomogeneity of the scattering length induced, e.g., by properly chosen external magnetic fields is an effective way to control the dynamics of matter-wave solitons.

ACKNOWLEDGMENTS

This work was supported by the "A.S. Onasis" Public Benefit Foundation (G.T.) and the Special Research Account of Athens University (G.T., D.J.F.), as well as Grant No. NSF-DMS-0204585, NSF-CAREER, and the Eppley Foundation for Research (P.G.K.).

[1] F. Dalfovo, S. Giorgini, L. P. Pitaevskii, and S. Stringari, Rev. Mod. Phys. **71**, 463 (1999).

[2] S. Burger, K. Bongs, S. Dettmer, W. Ertmer, K. Sengstock, A. Sanpera, G. V. Shlyapnikov, and M. Lewenstein, Phys. Rev. Lett. **83**, 5198 (1999); J. Denschlag, J. E. Simsarian, D. L. Feder, C. W. Clark, L. A. Collins, J. Cubizolles, L. Deng, E. W. Hagley, K. Helmerson, W. P. Reinhardt, S. L. Rolston, B. I. Schneider, and W. D. Phillips, Science **287**, 97 (2000); B. P. Anderson, P. C. Haljan, C. A. Regal, D. L. Feder, L. A. Collins, C. W. Clark, and E. A. Cornell, Phys. Rev. Lett. **86**, 2926 (2001); Z. Dutton, M. Budde, Ch. Slowe, and L. V. Hau, Science **293**, 663 (2001).

[3] K. E. Strecker, G. B. Partridge, A. G. Truscott, and R. G. Hulet, Nature (London) **417**, 150 (2002).

[4] L. Khaykovich, F. Schreck, G. Ferrari, T. Bourdel, J. Cubizolles, L. D. Carr, Y. Castin, and C. Salomon, Science **296**, 1290 (2002).

[5] B. Eiermann, Th. Anker, M. Albiez, M. Taglieber, P. Treutlein, K.-P. Marzlin, and M. K. Oberthaler, Phys. Rev. Lett. **92**, 230401 (2004).

[6] R. Folman, P. Krueger, J. Schmiedmayer, J. Denschlag, and C. Henkel, Adv. At., Mol., Opt. Phys. **48**, 263 (2002); J. Reichel, Appl. Phys. B: Lasers Opt. **75**, 469 (2002); J. Fortagh and C. Zimmermann, Science **307**, 860 (2005).

[7] B. A. Malomed, Prog. Opt. **43**, 71 (2002); A. V. Buryak, P. Di Trapani, D. V. Skryabin, and S. Trillo, Phys. Rep. **370**, 63 (2002).

[8] Yu. S. Kivshar and B. Luther-Davies, Phys. Rep. **298**, 81 (1998); P. G. Kevrekidis, K. Ø. Rasmussen, and A. R. Bishop, Int. J. Mod. Phys. B **15**, 2833 (2001).

[9] J. Weiner, *Cold and Ultracold Collisions in Quantum Microscopic and Mesoscopic Systems* (Cambridge University Press, Cambridge, England, 2003).

[10] S. Inouye, M. R. Andrews, J. Stenger, H. J. Miesner, D. M. Stamper-Kurn, and W. Ketterle, Nature (London) **392**, 151 (1998); J. Stenger, S. Inouye, M. R. Andrews, H.-J. Miesner, D. M. Stamper-Kurn, and W. Ketterle, Phys. Rev. Lett. **82**, 2422 (1999).

[11] J. L. Roberts, N. R. Claussen, J. P. Burke, Jr., C. H. Greene, E. A. Cornell, and C. E. Wieman, Phys. Rev. Lett. **81**, 5109 (1998); S. L. Cornish, N. R. Claussen, J. L. Roberts, E. A. Cornell, and C. E. Wieman, *ibid.* **85**, 1795 (2000).

[12] M. Olshanii, Phys. Rev. Lett. **81**, 938 (1998); T. Bergeman, M. G. Moore, and M. Olshanii, *ibid.* **91**, 163201 (2003).

[13] M. Theis, G. Thalhammer, K. Winkler, M. Hellwig, G. Ruff, R. Grimm, and J. H. Denschlag, Phys. Rev. Lett. **93**, 123001 (2004).

[14] J. Herbig, T. Kraemer, M. Mark, T. Weber, C. Chin, H. C. Nagerl, and R. Grimm, Science **301**, 1510 (2003).

[15] M. Bartenstein, A. Altmeyer, S. Riedl, S. Jochim, C. Chin, J. Hecker Denschlag, and R. Grimm, Phys. Rev. Lett. **92**, 203201 (2004).

[16] F. Kh. Abdullaev, J. G. Caputo, R. A. Kraenkel, and B. A. Malomed, Phys. Rev. A **67**, 013605 (2003); H. Saito and M. Ueda, Phys. Rev. Lett. **90**, 040403 (2003); G. D. Montesinos, V. M. Pérez-García, and P. J. Torres, Physica D **191**, 193 (2004).

[17] P. G. Kevrekidis, G. Theocharis, D. J. Frantzeskakis, and B. A. Malomed, Phys. Rev. Lett. **90**, 230401 (2003); D. E. Pelinovsky, P. G. Kevrekidis, and D. J. Frantzeskakis, *ibid.* **91**, 240201 (2003); F. Kh. Abdullaev, A. M. Kamchatnov, V. V. Konotop, and V. A. Brazhnyi, *ibid.* **90**, 230402 (2003); Z. Rapti, G. Theocharis, P. G. Kevrekidis, D. J. Frantzeskakis, and B. A. Malomed, Phys. Scr. **T107**, 27 (2004); D. E. Pelinovsky, P. G. Kevrekidis, D. J. Frantzeskakis, and V. Zharnitsky, Phys. Rev. E **70**, 047604 (2004); Z. X. Liang, Z. D. Zhang, and W. M. Liu, Phys. Rev. Lett. **94**, 050402 (2005).

[18] F. Kh. Abdullaev and M. Salerno, J. Phys. B **36**, 2851 (2003).

[19] H. Xiong, S. Liu, M. Zhan, and W. Zhang, e-print cond-mat/0411212.

[20] A. J. Moerdijk, B. J. Verhaar, and A. Axelsson, Phys. Rev. A **51**, 4852 (1995).

[21] Yu. S. Kivshar and B. A. Malomed, Rev. Mod. Phys. **61**, 763 (1989).

[22] Yu. S. Kivshar and X. Yang, Phys. Rev. E **49**, 1657 (1994).

[23] V. M. Pérez-García, H. Michinel, and H. Herrero, Phys. Rev. A **57**, 3837 (1998).

[24] V. E. Zakharov and A. B. Shabat, Zh. Eksp. Teor. Fiz. **61**, 118 (1971) **34**, 62 (1971)].

[25] J. Yan, Y. Tang, G. H. Zhou, and Z. H. Chen, Phys. Rev. E **58**, 1064 (1998).

[26] T. Hartmann, F. Keck, H. J. Korsch, and S. Mossmann, New J. Phys. **6**, 2 (2004).

[27] J. Satsuma and N. Yajima, Suppl. Prog. Theor. Phys. **55**, 284 (1974).

[28] W. Kohn, Phys. Rev. **123**, 1242 (1961).

[29] U. Al Khawaja, H. T. C. Stoof, R. G. Hulet, K. E. Strecker, and G. B. Partridge, Phys. Rev. Lett. **89**, 200404 (2002).

[30] D. J. Frantzeskakis, G. Theocharis, F. K. Diakonos, P. Schmelcher and Yu. S. Kivshar, Phys. Rev. A **66**, 053608 (2002).

[31] V. E. Zakharov and A. B. Shabat, Zh. Eksp. Teor. Fiz. **64**, 1627 (1973) [Sov. Phys. JETP **37**, 823 (1973)].

[32] Th. Busch and J. R. Anglin, Phys. Rev. Lett. **84**, 2298 (2000).

[33] G. Huang, J. Szeftel, and S. Zhu, Phys. Rev. A **65**, 053605 (2002).

[34] V. A. Brazhnyi and V. V. Konotop, Phys. Rev. A **68**, 043613 (2003); V. V. Konotop and L. Pitaevskii, Phys. Rev. Lett. **93**, 240403 (2004).

[35] D. E. Pelinovsky, D. J. Frantzeskakis, and P. G. Kevrekidis, Phys. Rev. E **72**, 016615 (2005).

[36] G. Huang, M. G. Velarde, and V. A. Makarov, Phys. Rev. A **64**, 013617 (2001); G. Huang, V. A. Makarov, and M. G. Velarde, *ibid.* **67**, 023604 (2003).

[37] N. G. Parker, N. P. Proukakis, M. Leadbeater, and C. S. Adams, Phys. Rev. Lett. **90**, 220401 (2003); N. P. Proukakis, N. G. Parker, D. J. Frantzeskakis, and C. S. Adams, J. Opt. B: Quantum Semiclassical Opt. **6**, S380 (2004).